# Dynamical behavior of thin ferroelectric liquid-crystal films in ac electric fields

W. S. Lo and Robert A. Pelcovits
*Department of Physics, Brown University, Providence, Rhode Island 02912*

R. Pindak and G. Srajer
*AT&T Bell Laboratories, Murray Hill, New Jersey 07974*

(Received 16 January 1990)

We study both experimentally and theoretically the behavior of a freely suspended ferroelectric smectic-$C^*$ liquid-crystal film in the presence of an ac electric field. The field drives the system periodically between two ordered phases with opposite polarization. We find several different regimes of dynamical behavior depending on the strength of the field. These results are explained in terms of a phenomenological free energy.

Much attention has been devoted to the dynamical properties of systems quenched from a disordered phase to a low-temperature ordered phase.[1] Of prime interest is the temporal evolution of the system to its final equilibrium ordered state. While most quenches are done in a single step and not repeated, it is also possible to impose a periodic quench, driving the system continuously between the disordered and ordered phases.[2] In this Brief Report we study a system that can be driven periodically between two *ordered* phases characterized by equal and opposite values of the order parameters. Our system is a freely suspended chiral smectic-$C^*$ liquid-crystal film in the presence of an extended applied ac electric field. The chiral smectic-$C^*$ phase is a layered phase in which the rod-shaped molecules have an average tilt angle $\theta_T$ from the layer normal. If the layer normal is taken to be in the $\hat{\mathbf{z}}$ direction, then the projection of the molecular tilt direction onto the layer planes can be characterized by a vector $\hat{\mathbf{c}}(x,y)$, called the "director," or, equivalently, by the angle $\phi(x,y)$ which $\mathbf{c}$ makes with the $x$ axis. The length of $\mathbf{c}$ is equal to $\sin\theta_T$. There also exists a local in-plane spontaneous polarization $\mathbf{P}(x,y)$ oriented perpendicular to $\mathbf{c}$, which couples directly to an external applied electric field.

Our experiment was performed on a three-layer film of the chiral liquid-crystalline material (*S*)-4-(2′-methylbutyl)phenyl 4′-(*n*-octyl)biphenyl-4-carboxylate (8SI). Previous work[3,4] has shown that the phase sequence of this compound is smectic $A$–smectic $C^*$–hexatic $I^* \rightarrow$hexatic $F^* \rightarrow$crystal $J^* \rightarrow$crystal $G^*$. Free-standing films were drawn across a $3\times9$ mm$^2$ rectangular hole in a 0.15-mm-thick glass slide. Electrodes were made by evaporating chromium and gold along the longer edge of the hole. The sample holder was placed in an oven with 10-mK temperature stability and optical access. Experiments were done at 85 °C, where the three-layer film was in the smectic-$C^*$ phase. Single-domain samples were obtained by applying a constant 1-kG magnetic field at a 45° angle from the normal to the film. The projection of the magnetic field onto the plane of the film is oriented along the $y$ axis while the electric fields are applied parallel to the $x$ axis. Depolarized reflected light microscopy was used to study the temporal and spatial variation of the molecular orientation. Films were illuminated with nearly normally incident polarized light of intensity $\sim$ 300 mW from an argon-ion laser. The reflected light was imaged through a nearly crossed analyzer onto the face of a charge-coupled-device (CCD) camera (Pulnix TM-845). Variations in the intensity of the resulting images are directly related to spatial variations in the molecular director. This is because the reflected-light polarization vector will be rotated toward the local optic axis which, for the material studied, coincides with the local director orientation.[5] To study the temporal evolution of the spatial director patterns, a video tape recorder was connected to the camera. Subsequently, selected time sequences were transferred onto an optical disk (Panasonic TQ-2082F) for further analysis. For an applied sinusoidal ac field of 10 Hz, six spatial patterns could be observed per cycle. As a function of the amplitude of the applied field, four distinct regimes of director reorientation were observed (see Fig. 1). In the first regime [Fig. 1(a)], occurring for voltage amplitudes less than about 10 V peak-to-peak, the film exhibits a single $\pi$-disclination wall separating two domains of opposite polarization. This wall oscillates back and forth in phase with the field, with the local polarization in the larger domain in alignment with the field direction. The presence of the $\pi$ wall can be understood by noting that in the absence of any electromagnetic fields, the sample, when drawn, will have a $2\pi$-point disclination at its center due to the parallel molecular alignment with the boundaries. The applied magnetic field will drive this singularity to the edge of the sample leaving a bendlike pattern of molecular orientation or a corresponding splaylike pattern of the local polarization with the local polarization pointing in the $y$ direction along the center line of the sample. This line will then be the core of a $\pi$ wall which will oscillate back and forth in phase with the electric field. At higher voltages ($\sim$40 V), see Fig. 1(b), new behavior is observed: the single $\pi$-disclination wall is gone, and islands appear in which the local polarization is oriented in the opposite direction to the local polarization in the surrounding region. The interface between the islands and the surrounding region (referred to as the background) are then $\pi$-disclination walls. Halfway

 

through the cycle, the background switches its direction of polarization; new islands appear with polarization opposite to that of the background. As the voltage is increased ($\sim 120$ V), see Fig. 1(c), yet a new regime is observed: the islands are now replaced by a network of $2\pi$-disclination walls which separate domains with the *same* direction of polarization. During successive cycles the $2\pi$ walls grow in number until reaching a spacing of $\sim 200$ $\mu$m. As the field varies in direction, the regions of opposite polarization at the center of the $2\pi$ walls expand resulting in new $2\pi$ walls appearing halfway between the original ones. The final regime [Fig. 1(d)] occurs for voltages exceeding about 600 V, where once again islands of opposite polarization appear as in the second regime above.

To explain the existence of the four regimes described above, we consider the following free-energy density for the smectic films, with director field **c**, transverse polarization **P**, magnetic field **H**, and ac field $\mathbf{E}(\omega)$:

$$F=-(\epsilon_a/8\pi)(\mathbf{c}\cdot\mathbf{E})^2-\mathbf{P}\cdot\mathbf{E}(\omega)-(\chi_a/2)(\mathbf{c}\cdot\mathbf{H})^2 . \quad (1)$$

In the above equation $\epsilon_a$ and $\chi_a$ are the dielectric and magnetic susceptibilities, respectively. The expression (1) neglects the elastic energy whose effect will be considered separately below. We also neglect contributions from free ions since the relaxation time in the film for a charge distribution of characteristicize $L$ is slower than the bulk charge relaxation time by a factor of $L/h$, where $h=10^{-6}$ cm is the film thickness.[5] For the 200-$\mu$m features observed, free ion motion is a factor of 200 slower than typical 10-msec bulk charge relaxation times and hence is negligible at 10 Hz.

Assuming an average molecular tilt angle $\theta_T$ and an applied **E** field parallel to the $x$ direction we can rewrite

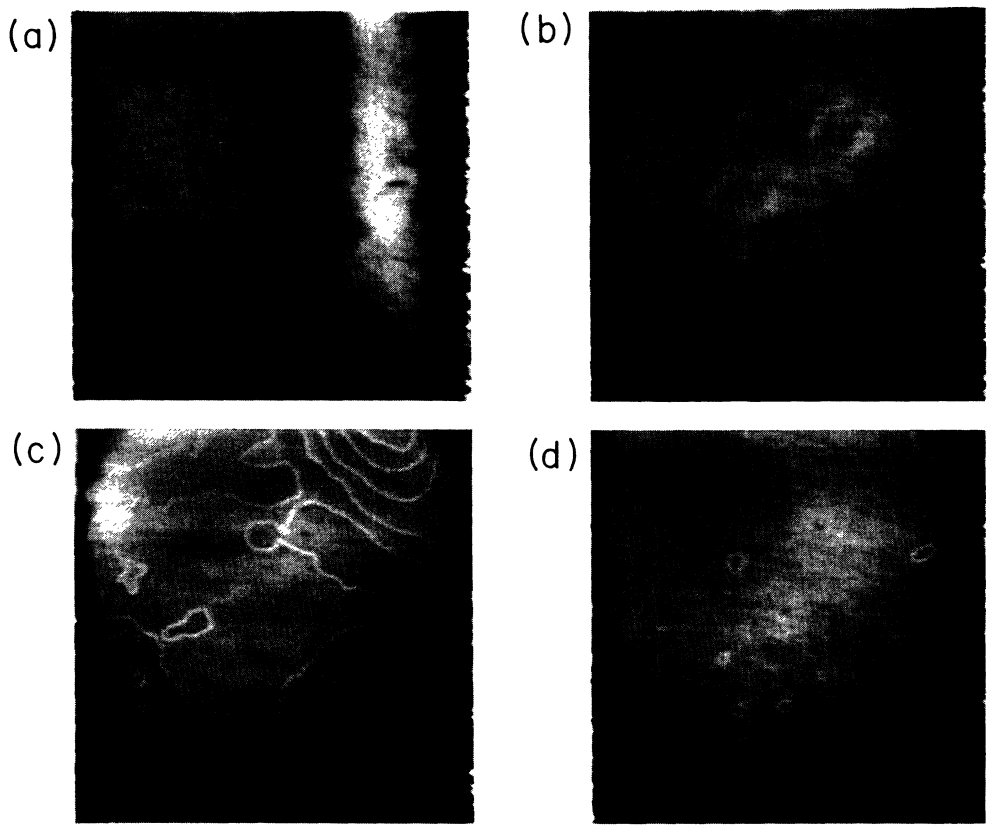


FIG. 1. Polarized photomicrographs of four distinct director reorientation regimes as a function of applied voltage. The direction of the applied 10-Hz ac field is horizontal and the direction of the magnetic field projection onto the plane of the photograph is vertical. The long edges of the rectangular hole, spaced apart by 3 mm, are visible at the left and right sides of the photographs. Photo (a) was taken in the first regime ($V=10$ V). Two domains of opposite polarization, separated by a $\pi$-disclination wall, are observed. The domain on the left side has a polarization reorientation favored by the electric field and is thus larger. Photo (b) was taken in the second regime ($V=40$ V). This regime is characterized by the appearance of isolated islands separated by $\pi$ walls from a uniform background. When the applied field is reversed the existing islands disappear and the new islands are formed in the intermediate region. Photo (c) was taken in the third regime ($V=120$ V). In this regime domains of the same polarization are observed separated by long, irregular $2\pi$ walls. When the applied field reverses direction, the existing $2\pi$ walls expand forming new $2\pi$ walls at locations approximately halfway between their former locations. Finally, photo (d) was taken in the fourth regime ($V=600$ V). This regime is analogous to the second regime [photo (b)]. The only difference is that the size of the islands is smaller than in (b). Note, when imaged through a nearly crossed analyzer, the $\pi$ wall consists of both a light and dark stripe each of which becomes more visible at different times in the applied field cycle. Photos (b) and (d) were taken at such different times and hence their seemingly different appearance.

(1) in polar coordinates as follows:

$$F=F_1+F_2+F_3\ , \tag{2a}$$

$$F_1=-(\epsilon_a/8\pi)\sin^2\theta_T(E_0\cos\omega t)^2\sin^2\phi\ , \tag{2b}$$

$$F_2=-P_0E_0\sin\theta_T\cos\omega t\cos\phi\ , \tag{2c}$$

$$F_x=-(\chi_a/2)H^2\cos^2\phi\ , \tag{2d}$$

where

$$\mathbf{P}=P_0\hat{\mathbf{z}}\times\mathbf{c}=P_0\sin\theta_T(\hat{\mathbf{x}}\cos\phi+\hat{\mathbf{y}}\sin\phi),\quad \mathbf{E}=\hat{\mathbf{x}}E_0\cos\omega t\ . \tag{3}$$

The three contributions to $F$ are plotted as a function of $\phi$ in Fig. 2.

We have measured $\epsilon_a$ in the nematic- and smectic-$A$ phases of the racemate of 8SI using surface-aligned sample cells of the bulk material. At the high-temperature end of the nematic phase, $\epsilon_a$ is found to be positive and of magnitude 0.5, but decreases in value with decreasing temperature. Just above the $A$-$C^*$ transition, $\epsilon_a$ crosses over to being negative and, extrapolating our data into the $C^*$ phase to the temperature at which our measurements were done, we find $\epsilon_a\simeq-0.5$. To obtain a value for the three-layer film, we multiply this bulk value by the film thickness. Similarly for $\chi_a$, we estimate using typical bulk values that $\chi_a\sim5\times10^{-12}$ in the film. The transverse polarization $\mathbf{P}$ has been measured to be $1.0\times10^{-5}$ esu/cm in a three-layer film.[6] Due to the finite width of the electrodes, the electric field in the middle of the sample will be approximately equal to 0.66V/d.[7] With a film width of 3 mm, the applied *peak-to-peak* voltage $V$ is related to $E_0$ in cgs units, by $V\approx300E_0$. The magnetic field $H$ is 1 kG and $\theta_T\approx30°$.

The free energy $F$ can exhibit both a single-well and double-well structure depending on the relative strengths of $F_1$, $F_2$, and $F_3$. It is straightforward to show that a single well (located at $\phi=0$ or $\pi$, depending on the direction of $\mathbf{E}$) alone will exist for $E_-<E_0\cos\omega t<E_+$, where

$$E_-=\frac{\chi_aH^2}{P_0\sin\theta_T},\quad E_+=\frac{4\pi P_0}{|\epsilon_a|\sin\theta_T}\ . \tag{4}$$

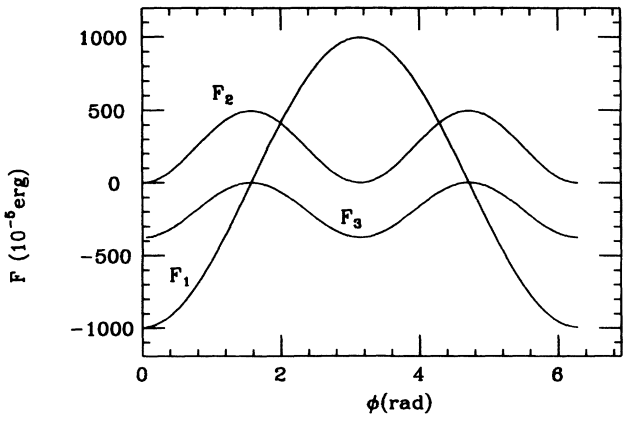


FIG. 2. Plots of the three contributions $F_1$, $F_2$, and $F_3$ to the total free energy Eq. (2a). We use the values of $\epsilon_a$, $P_0$, $\theta_T$, $\chi_a$, and $H$ discussed in the paragraph following Eq. (3), and set $E_0=1000$ statvolts/cm and $\omega t=0.1$. The value of $F_3$ has been multiplied by 1500 so that it will be discernible on this scale.

If we assume that these threshold values correspond to rms values of the applied field, then the peak-to-peak voltages corresponding to $E_-$ and $E_+$ are approximately 70 and $1.5\times10^5$ V. At fields lower than $E_-$ a double-well structure will appear, with the $F_2$ term biasing one of the two equal wells imposed by $F_3$ (the dielectric term $F_1$ is negligible at low fields). At fields higher than $E_+$,

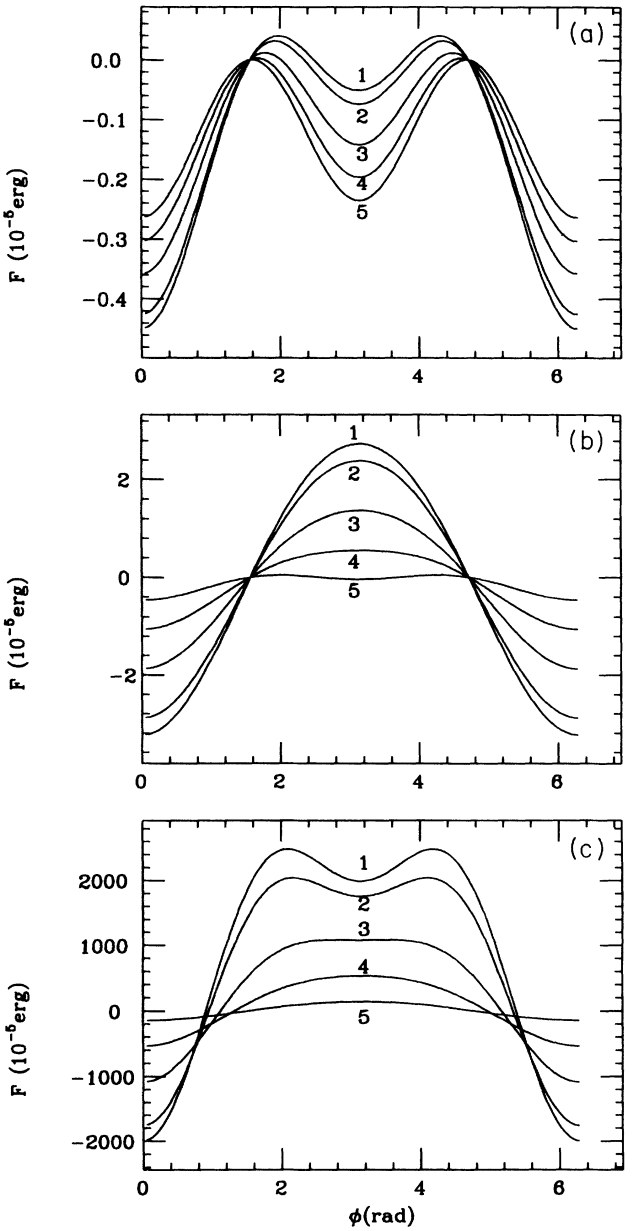


FIG. 3. Plots of free energy $F$ for three values of the electric-field amplitude for various values of time in one-half cycle of the field oscillation. The curves correspond to values of $\omega t$ as follows: (2) $\omega t=0.1$; (2) $\omega t=0.5$; (3) $\omega t=1.0$; (4) $\omega t=1.3$, and (5) $\omega t=1.5$. The field amplitudes are (a) $E_0=0.2$, (b) $E_0=3$, and (c) $E_0=2000$. Values of $E_0$ are in cgs units. (a) corresponds to $E_0<E_-$, (b) to $E_-<E_0<E_+$, and (c) to $E_0>E_+$, given by Eq. (4). The double-well structure with wells located at $\phi=0$ and $\pi$ is evident in (a) and (c), while (b) illustrates the single-well regime. In the subsequent half-cycle the well with lowest energy appears at $\phi=\pi$.

the $F_2$ term now biases one of the two wells imposed by $F_1$, the magnetic contribution $F_3$ being negligible. Plots of $F$ in these different field regimes are shown in Fig. 3.

We now discuss the origin of the four observed regimes of dynamical behavior. At low voltages [Fig. 1(a)], the electric-field correlation length $\xi_E = \sqrt{K/PE}$ is large.[8] Here $K$ is some combination of the bend and splay elastic constants, associated with the electric-field distortion of the $2\pi$ singularity driven to the edge of the sample by the $H$ field. The $\pi$ wall induced by the $E$ field will then oscillate back and forth. The domains of opposite polarization on either side of the wall are essentially coherent, and thermal fluctuations do not play an important role as first noted in Ref. 8. As the applied voltage is increased, $\xi_E$ drops in value. The threshold for Fig. 1(b) occurs when $\xi_E/d \approx 10^{-3}$, assuming $K \approx 10^{-12}$ erg,[9] at which point the domains of opposite polarization in Fig. 1(a) have certainly lost their coherence. This threshold value of $\xi_E/d$ is about a factor of 10 smaller than that observed in Ref. 8 for surface-stabilized ferroelectric liquid-crystal cells. From $E_t$ in Eq. (4) we see that $F$ exhibits a double-well structure up to about 70 V in good agreement with the observed threshold for Fig. 1(c). The droplets shown in Fig. 1(b) are presumably regions of polarization whose direction is opposite to that of the bulk of the sample and correspond to the metastable state provided by the upper well of $F$. The subsequent regime, Fig. 1(c), should correspond to the range of fields $E_- < E_{\rm rms} < E_+$ where only a single well exists in $F$. The network of domain walls in Fig. 1(c) is apparently $2\pi$ walls separating domains of identical polarization. The origin of these $2\pi$ walls has been explained in Ref. 8, where it is shown that thermal fluctuations give rise to domains with local polarization deviating slightly from the mean direction of the polarization. When the field switches these domains reorient, with the local polarization rotating clockwise or counterclockwise to follow the shortest angular path to the new equilibrium state. A $2\pi$ wall will arise then between two domains that reorient in opposite senses. The upper voltage limit for Fig. 1(c) should in theory be given by Eq. (4b), which is apparently in disagreement with the experimental data by several orders of magnitude, if we equate the threshold value with the rms value. At present, we have no explanation for this discrepancy. Nevertheless, the theory is certainly appealing on a qualitative level, as Fig. 1(d) is similar in appearance to Fig. 1(b). This observation is in accord with the reappearance of the double-well structure in $F$ at high voltages where the dielectric term $F_1$ dominates. We suspect that the lack of quantitative agreement between the theory and experiment for the upper voltage limit of Fig. 1(c) is due to our use of a *static* Landau theory (albeit with time-varying parameters). Ideally this problem should be analyzed with a complete dynamical theory, which is planned to be the subject of future work.

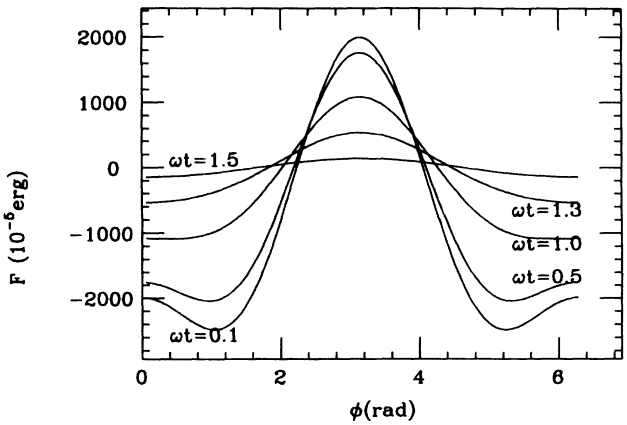


FIG. 4. The free energy $F$ as a function of $\phi$ when $\epsilon_a = 0.5$ and $E_0 = 2000$ ($E_0 > E_+$). The figure shows the presence of the double wells, which at the field maximum ($\omega t \approx 0$), are now located between $\phi = 0$ and $\pi/2$, and $\phi = 3\pi/2$ and $2\pi$. As the field decreases the wells move towards $\phi = 0$ and $2\pi$. At $\omega t$ slightly greater than $\pi/2$, these wells would reappear on either side of $\phi = \pi$ and then move outwards from that value as the field increases in strength.

Finally, we discuss what we expect to happen in a material where $\epsilon_a > 0$. At low fields the dielectric energy $F_1$ is negligible, so we expect that Figs. 1(a)–1(c) should be essentially unchanged. The threshold values Eqs. (4) are also unchanged. At high fields [i.e., the regime of Fig. 1(d)], the free energy will exhibit two wells of *equal* depth. This is illustrated in Fig. 4 with a time series of plots of $F$. We expect to see domains of polarization corresponding to the two wells, which will be separated by low-angle walls, since the wells are closely spaced at fields close to $E_+$. As a function of time these walls will disappear as the field passes through zero and reappear again as the field changes sign. Currently, experiments are underway on a material with positive $\epsilon_a$, *p*-decyloxybezylidene *p'*-amino-2-methylbutylcinnamate (DOBAMBC) to check these assertions.

We are indebted to Noel Clark for helpful discussions and furnishing us with a copy of Ref. 8, and to Tapio Ala-Nissila for helpful discussions. W.S.L. and R.A.P. were supported by the National Science Foundation under Grant No. DMR86-03536.

[1]See, e.g., J. D. Gunton, M. San Miguel and P. S. Sahni, in *Phase Transitions and Critical Phenomena,* edited by C. Domb and J. L. Lebowitz (Academic, London, 1983), Vol. 8.

[2]M. Joshua, W. I. Goldburg, and A. Onuki, Phys. Rev. Lett. **54**, 1175 (1985); A. Onuki, Prog. Theor. Phys. **66**, 1230 (1981).

[3]J. Budai, R. Pindak, S. C. Davey, and J. W. Goodby, J. Phys. (Paris) Lett. **45**, L1053 (1984).

[4]S. Gierlotka, J. Przedmojski, and B. Pura, Liq. Crys. **3**, 1535 (1988).

[5]R. Pindak, C. Y. Young, R. B. Meyer, and N. A. Clark, Phys. Rev. Lett. **45**, 1193 (1980).

[6]S. B. Dierker and R. Pindak, Phys. Rev. Lett. **59**, 1002 (1987).

[7]C. Rosenblatt, Ph.D. thesis, Harvard University, 1979 (unpublished).

[8]J. E. Maclennan, Ph.D. thesis, University of Colorado, 1988 (unpublished).

[9]C. Rosenblatt, R. B. Meyer, R. Pindak, and N. A. Clark. Phys. Rev. A **21**, 140 (1980).

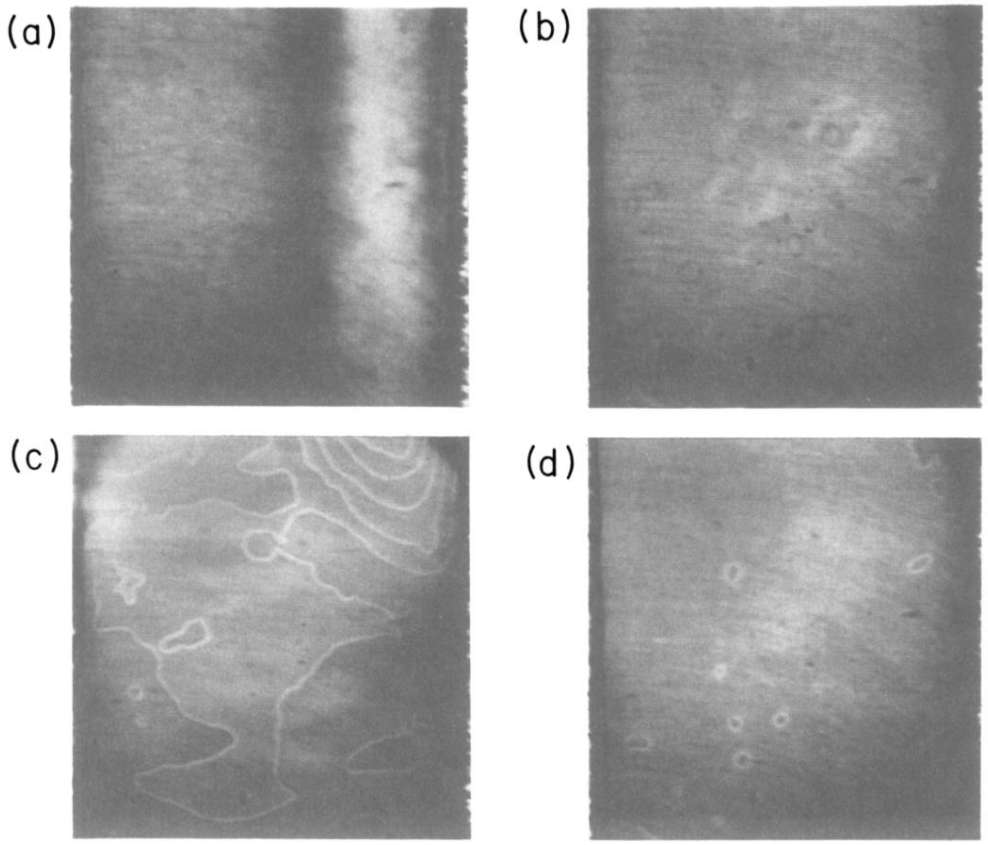


FIG. 1. Polarized photomicrographs of four distinct director reorientation regimes as a function of applied voltage. The direction of the applied 10-Hz ac field is horizontal and the direction of the magnetic field projection onto the plane of the photograph is vertical. The long edges of the rectangular hole, spaced apart by 3 mm, are visible at the left and right sides of the photographs. Photo (a) was taken in the first regime ($V=10$ V). Two domains of opposite polarization, separated by a $\pi$-disclination wall, are observed. The domain on the left side has a polarization reorientation favored by the electric field and is thus larger. Photo (b) was taken in the second regime ($V=40$ V). This regime is characterized by the appearance of isolated islands separated by $\pi$ walls from a uniform background. When the applied field is reversed the existing islands disappear and the new islands are formed in the intermediate region. Photo (c) was taken in the third regime ($V=120$ V). In this regime domains of the same polarization are observed separated by long, irregular $2\pi$ walls. When the applied field reverses direction, the existing $2\pi$ walls expand forming new $2\pi$ walls at locations approximately halfway between their former locations. Finally, photo (d) was taken in the fourth regime ($V=600$ V). This regime is analogous to the second regime [photo (b)]. The only difference is that the size of the islands is smaller than in (b). Note, when imaged through a nearly crossed analyzer, the $\pi$ wall consists of both a light and dark stripe each of which becomes more visible at different times in the applied field cycle. Photos (b) and (d) were taken at such different times and hence their seemingly different appearance.